Anat Embryol (1988) 178:309–326

Anatomy
and Embryology

Pre-natal development of rat nasal epithelia

IV. Freeze-fracturing on apices, microvilli and primary and secondary cilia of olfactory and respiratory epithelial cells, and on olfactory axons

Bert Ph. M. Menco

Department of Neurobiology and Physiology, O.T. Hogan Hall, Northwestern University, Evanston, IL 60208, USA

Summary. Olfactory axons and apical structures of olfactory epithelia and of nasal respiratory epithelia of rat embryos were studied with the freeze-fracture technique; adult tissue samples of the same sources were used for comparison. At the onset of epithelial differentiation (14th gestational day) intramembranous particle densities are the same for all structures in both epithelial types. During further development, particle densities in membranes of primary cilia remain lower than those in membranes of other apical structures. Otherwise, I found the following from the 14th to the 19th day of gestation. *a. Olfactory receptor cells* of embryos of all age groups have axons wherein the membrane particle densities are about half those of adults. These densities are always lower than those of dendritic ending structures. Dendritic endings with primary cilia have lower densities than endings with secondary cilia; densities mainly increase when the endings sprout secondary cilia. Adult values are reached at the 18th day of gestation. *b. Olfactory supporting cells* with only globular particles in their apices gradually transform into, or are replaced by, supporting cells which also have dumbbell-shaped particles in their apices. Particle densities are always higher in apical structures of supporting cells than in apical structures of receptor cells. Adult values are reached at the 17th day of gestation. *c. Putative ciliated and ciliated respiratory epithelial cells* have considerably lower particle densities in membranes of their apical structures than do olfactory epithelial cells. Of special interest is that this is also true for secondary respiratory and olfactory cilia; as soon as genesis of secondary cilia in either epithelial type begins, their membrane features differ. Also, in contrast to apical structures of the olfactory epithelium, particle densities in apical structures of the respiratory epithelium do not systematically change during pre-natal development, and resemble the density values of adults. An exception are the microvilli of the respiratory cells with secondary cilia, membranes of which have considerably higher particle densities in adults than in embryos. In conclusion: Transformations of olfactory receptor cell dendritic endings with primary cilia into endings with secondary cilia, and of olfactory supporting cells with globular particles in their apices into cells with dumbbell-shaped particles in their apices are accompanied by increases in the densities of their intramembranous particles. These developmental changes parallel the electrophysiological onset of olfactory receptor cell specificity.

Key words: Axons – Cilia – Microvilli – Olfactory – Respiratory – Development – Freeze-fracturing – Rat

Introduction

Electrophysiological studies on olfactory epithelia of rat embryos suggest that a population of receptor cells, each of which responds to all odorants administered, transforms during development into a population of cells each of which responds preferentially to a limited set of odorants, i.e., into a population that displays receptor cell specificity (Gesteland et al. 1982). This transformation occurs simultaneously with the development of an epithelium consisting of receptor cells having secondary cilia from one having only primary cilia (Menco and Farbman 1985a, b). Furthermore, extensive freeze-fracture and -etch studies in a number of vertebrate species demonstrated that secondary olfactory cilia have higher densities of membrane-associated particles than secondary cilia of the non-sensory nasal respiratory epithelium that borders the olfactory one (Kerjaschki and Hörandner 1976; Menco 1977, 1980a, b, 1983, 1984; Menco et al. 1976; Usukura and Yamada 1978; Breipohl et al. 1982). As mature olfactory receptor cells in vertebrates have only secondary cilia (Menco and Farbman 1985a, b), these presumably contain the receptor sites to odorous stimuli. Freeze-fracture and -etch particles are likely candidates for olfactory receptor and/or transducer molecules (Getchell 1986; Holley and MacLeod 1977; Lancet 1986; Menco 1983, 1984).

The present study, which forms part of a series dealing with freeze-fracture features of developing nasal epithelia (Menco 1988a, b), concerns the membrane features accompanying overall morphological and electrophysiological developmental transformations during the rat's embryonic development. It includes the first systematic freeze-fracture morphological investigation on primary cilia. Three preliminary reports have appeared (Menco 1987a, b; Menco and Minner 1986).

Materials and methods

Animal choice and sample preparation

E14 and E16 through E19 embryos (E1 = day that the dams were sperm-positive, E23 = P1, day of birth) of the Sprague Dawley rat (Holtzman Co., Madison, Wisconsin) were used for this investigation, employing 70 embryos per age group. For each age group 8 dams were killed by CO_2 asphyxiation. Nasal septa of the embryos and of 5 adults, which served as comparison material, were fixed in Karnovsky's (1965) aldehyde fixative in 0.1 M Na cacodylate, pH 7.4, at room temperature for 3 h, washed in buffer, cryo-pro-

tected with buffered 30% glycerol for 2 h and frozen in liquid propane. The samples were knife-fractured in a Cressington CFE 40 freeze-fracture machine (Cressington Scientific, Watford, U.K.) at a vacuum better than 10^{-6} mbar and at a temperature of $-150°$ C. Fractured specimens were rotary-replicated (300 rpm) with platinum/carbon or, sometimes, with tantalum/tungsten at angles of 20°. The latter method yields a smaller grain size and the replication material is more homogeneously distributed than with platinum/carbon evaporation (Menco et al. 1988; compare Fig. 12 with Figs. 11 and 13 using a magnifying glass). Replicas were reinforced with carbon obliquely evaporated from above. They were cleaned in 40% chromic acid and examined on uncoated 300 mesh hexagonal grids at 100 kV in a JEOL 100 CX Temscan electron microscope equipped with a eucentric goniometer. Stereopairs were made at angles of $\pm 6°$. The micrographs were printed in reverse contrast, and fracture planes were labelled according to Branton et al. (1975).

Data evaluation

Numbers of useful replicas were small considering the number of embryos; the fracture planes often did not include the required features. Each observation of a particular structure was based on one micrograph; numbers of observations equate those of micrographs used. These numbers ranged from 1 to 70, but were between 5 and 30 for most structures, and between 3 and 10 for primary cilia. For reasons of clarity, numbers of observations are not presented in Figs. 23–26; Tables 1 and 2 take these numbers into account. Particle counts were carried out at final magnifications of X 90000 to X 150000 using a grid ruled in 1 cm^2 divisions (Menco 1980b). I gathered information on densities of intramembranous particles but not on their diameters. With the exception of dumbbell-shaped particles of supporting cells (Figs. 7, 16), diameters of particles in the structures of interest show few differences using Pt/C replication. They are usually between 8 and 10 nm (Menco 1980b, 1983, 1984). Statistics included standard errors of means and one-, two-, and three-way analyses of variance (ANOVAs). They were compiled with a Macintosh$^+$ microcomputer and the Statview 512$^+$ (Brainpower, Inc., Calabasas, California) statistical package. Tables 1 and 2 do not include comparisons insignificant at levels of $p < 0.05$, but these are discussed in the text. I compromised for the statistics: not all structures occur (e.g., secondary respiratory cilia in age groups younger than E18 in Figs. 25 and 26), and not all of them were encountered in every age group (e.g., primary cilia of supporting cell Type A at E18 in Fig. 24).

Results

Freeze-fracture features at the onset of epithelial differentiation

At E14 olfactory and respiratory epithelia of the rat begin to differentiate. Just before the onset of differentiation, the surface appearances of the two epithelia resemble each other; both have few appendages other than primary cilia. Microvilli were rarely seen (Figs. 1–3; Figs. 1, 2, Menco 1988b). Differentiating E14 epithelial surfaces assume characteristics of mature olfactory and respiratory epithelia (Figs. 4–22; Figs. 3–15, Menco 1988b). E14 embryos displaying the latter features were labelled E14.2, whereas E14 embryos displaying the undifferentiated epithelial surface features were named E14.1 (Menco and Farbman 1985a, 1987).

Olfactory receptor cells

Not all olfactory receptor cells display primary cilia on their surfaces; in fact they may have no cilia whatsoever. This is true for cells in undifferentiated (Fig. 1) and differentiating olfactory epithelia (Figs. 4–6). Initially the knob-shaped dendritic endings of the olfactory receptor cells often occur in clusters (Figs. 5, 6; Menco and Farbman 1985a, b). Cells with secondary olfactory cilia were seen from E16 on (Figs. 8, 23). Newly formed secondary cilia are rather short and, like primary cilia (Fig. 3), have club-shaped (Fig. 8) ends. Distal parts of olfactory cilia were only occasionally seen at E16 and E17 (Fig. 6) and more frequently at E18 and E19 (Fig. 10). From here on *primary endings* and *secondary* endings indicate olfactory receptor cell dendritic endings without cilia as well as those with one cilium, and cells with secondary cilia, respectively.

Intramembranous particle densities in P- and E-faces of axons, dendritic endings, and primary and secondary cilia of olfactory receptor cells were compared for pre-natal age groups E14, E16–E19, and adults (Fig. 23; Table 1, I–V). E-face densities are always lower than those in P-faces (Figs. 5, 9, 10, 23). As particle distributions in proximal and distal parts of secondary olfactory cilia are the same, these were pooled in Figs. 23 and 26–29. Densities tend to be significantly lower in primary than in secondary endings (Table 1, II) and increase with development (Figs. 4–10, 23; Table 1, "age" effects in II–V, especially III and V). In the case of both primary and secondary endings, particle densities of endings and cilia tend not to differ (Fig. 23; Table 1, III, V, "structure" effects not significant, apart for E-faces secondary endings). Densities stabilize around E18 when, especially for secondary endings (Figs. 23, 27), they match those in adults; from E18 on I found no

Fig. 1. Olfactory epithelial surface of an E14.1 rat embryo with undifferentiated cells. The narrow and bulging profiles at the top suggest that these would have become receptor cells. One primary cilium extends from a membranous pouch (*large arrow*); another one is obliquely fractured (*small arrow*). Particle densities in P-(*PF*) and E-faces (*EF*) are low. The epithelial surface shows tricellular (*open arrow*), but no bicellular tight-junctional strands. × 30000

Fig. 2. Stereopair of the area of the previous micrograph where a primary cilium emerges from a membranous pouch. The pouch displays an E-face (*EF*); the cilium a P-(*PF*) and E-face. Particle densities are low. × 100000

Fig. 3. E14.1 olfactory receptor cell primary cilium, pointing downward and also emerging from a pouch. The cilium has a club-shaped tip (*arrow*). The pouch displays an E-face and the cilium a P-face. Particle densities are low. × 100000


EF
EF
PF
1

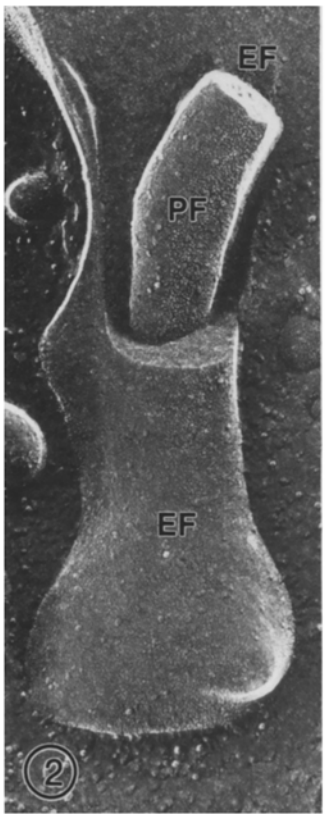
EF
PF
EF
2

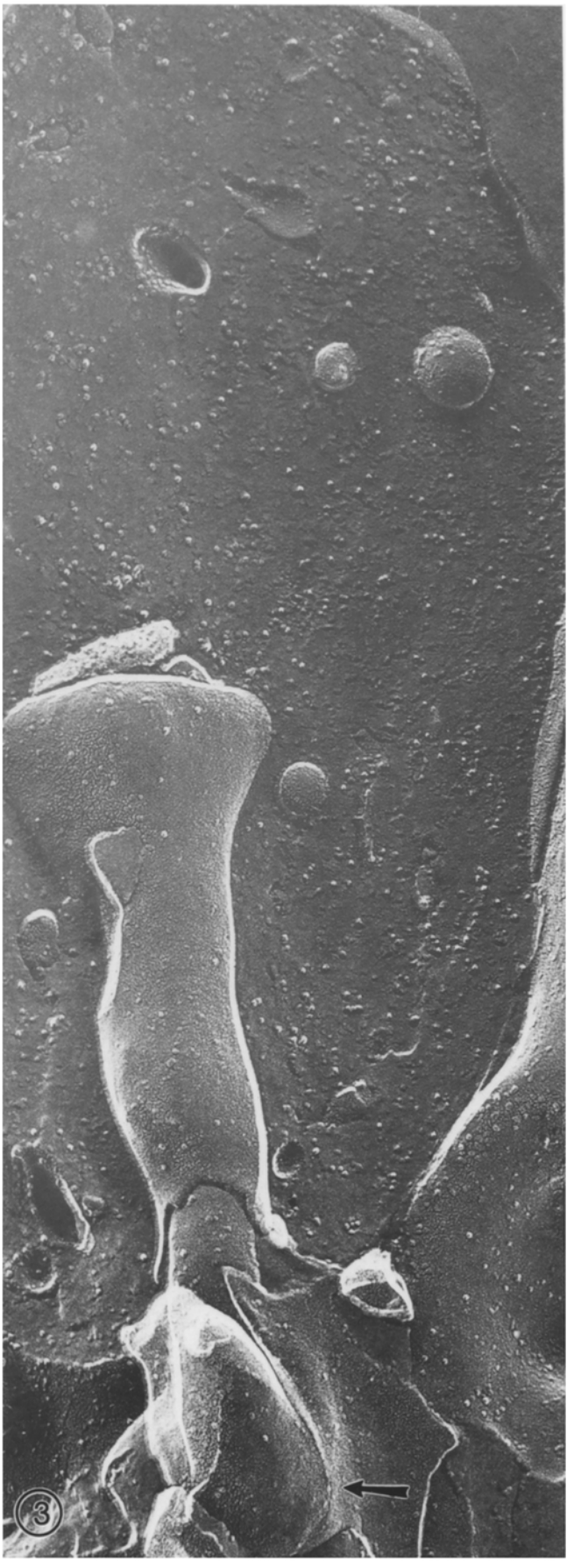
3

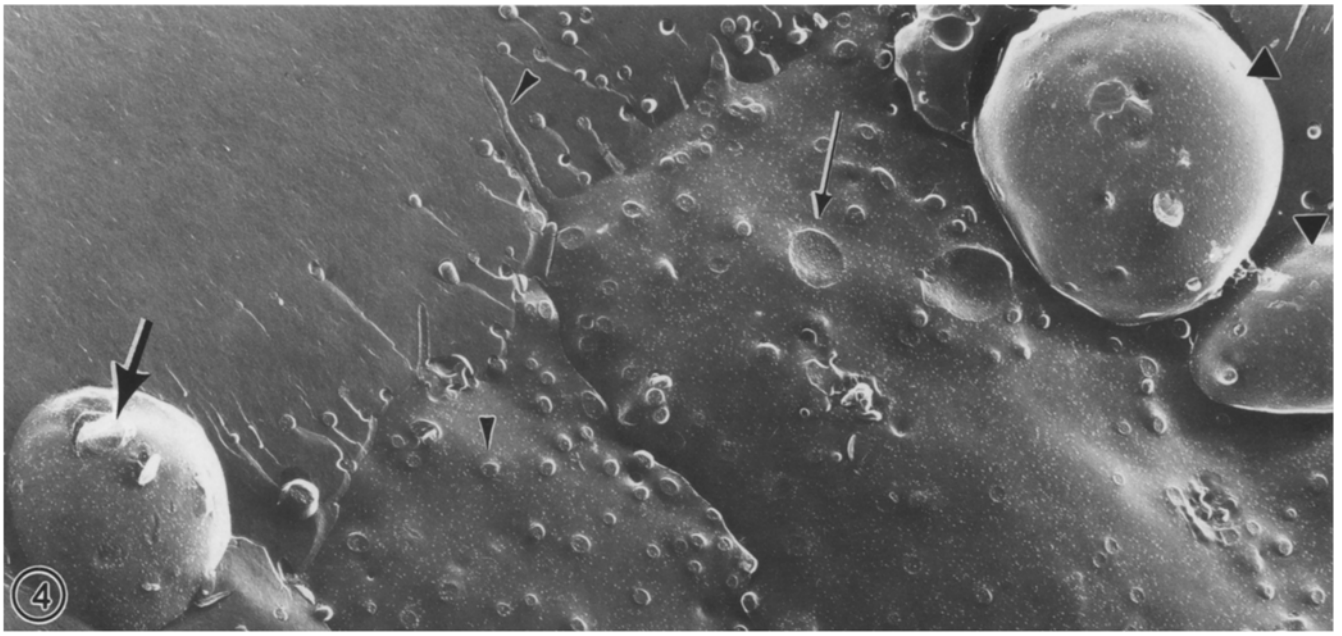
4


5

more "age" effects (Table 2, VI). Pooled over both fracture faces, densities range from 600 particles/μm^2 at E14 to 1400 particles/μm^2 from E18 on.

Particle arrays typical for genesis of primary or secondary cilia were seen in membranes of dendritic endings without cilia (Fig. 6) and with primary (Fig. 7) or secondary cilia (Fig. 8). For primary endings the arrays were seen from E14.2 on. For secondary ones (Fig. 8) their presence suggests that not all cilia form at the same time.

Axons of olfactory receptor cells

Olfactory receptor cell axons were observed from E14.1 on and have about the same diameter as the cilia (Menco 1980a). Hence, they provide a convenient region for comparison of densities of intramembranous particles with those of cilia. At E14.1 and E14.2 axonal and dendritic ending particle densities are similar (Fig. 23). P-face densities in axonal membranes of all embryonic age groups are about half those of adults (Figs. 11–13, 23; statistics not presented), i.e., 400 particles/μm^2 and 700 particles/μm^2, respectively, when pooled over P- and E-faces. This caused a significant p-value (Table 1, I).

Olfactory supporting cells

From E14.2 on, olfactory supporting cells begin to form microvilli (Figs. 4, 6–9, 14–16). Supporting cells with only globular particles (Type A; Figs. 4, 7, 8, 14) and supporting cells which also have rod- or dumbbell-shaped particles (Type B; Figs. 7, 15) were distinguished in regions above tight-junctions. The dumbbell-shaped particles are reflected as dumbbell-shaped pits in E-faces (Fig. 16, inset). In one fortunate E17 replica Type A and Type B supporting cells could clearly be seen to coexist (Fig. 7). Type A (Figs. 4, 7, 14) and B (Figs. 15, 16) supporting cells can have primary cilia in addition to microvilli. Dumbbell-shaped particles do not occur in these cilia and only occasionally in the microvilli. At E14 I saw only Type A supporting cells (Fig. 4). Type B supporting cells were seen from E16 on. About 40% of all supporting cells at E16 are of Type B. At E17 and E18 I encountered equal numbers of Type A and B supporting cells. At E19 about 80% have Type B characteristics, and in adults virtually all the cells are of Type B. For this I reexamined micrographs of adults of my previous investigations. Consequently, it appears that supporting cells with only globular particles (Type A) in their apices are replaced by, or transform into, olfactory supporting cells which also have dumbbell-shaped particles in their apices (Type B). This notion is further supported by the statistically significant interaction of three parameters examined – supporting cell type, age groups, and structures (Table 1, VI). Only Type A supporting cells show a significant density increase with age (Table 1, VI, VII), i.e., from 400 to 500 particles/μm^2 at E14.1 to 1500 to 2000 particles/μm^2 at E17 and older. From the earliest time I saw them – E16 – Type B supporting cells have adult particle density values (Fig. 24). Apices and microvilli in both supporting cell types have similar particle densities; those of primary cilia are lower, i.e., 200–900 particles/μm^2 (Fig. 24). This is the cause of the "structure" effect in Table 1, VIII (Fig. 15). Densities in primary cilia of Type A supporting cells also tend to be lower than those in apices and microvilli (Figs. 14, 24); that this effect is not significant may be due to lack of data.

Respiratory epithelia

After the onset of differentiation, at E14, and before they start to sprout cilia, at E18, respiratory epithelial cells have mainly microvilli and sometimes primary cilia (Figs. 17–19). Part of the respiratory cells belong to a type which remains microvillous throughout further development, and in adults; others become eventually ciliated. Cells with flat surfaces (Fig. 17) were characterized as *putative ciliated* (Menco and Farbman 1987, and references therein), whereas those with bulging surfaces were characterized as cells which remain *microvillous*. Apices of the latter cell type can have dumbbell-shaped particles (Figs. 19, 20). Secondary respiratory cilia were first seen at E18, but only on a few cells. Most of my observations on developing respiratory cilia were done in E19 embryos, as these had many more cells with secondary cilia. Cilia first appear as small stubs (Fig. 21), then become elongated and bat-shaped (Fig. 22).

At E14, especially E14.1, densities of intramembranous particles are lower than those in older embryos and in adults (Fig. 25). Membranes of apical structures of microvillous respiratory cells tend to have significantly higher densities (800–1200 particles/μm^2 from E16 on) than membranes of apical structures of putative ciliated cells (500–1000 particles/μm^2 from E14.2 on; Fig. 25; Table 1, IX). In both cell types these densities do not systematically change with developmental age (Fig. 25; Table 1, IX, "age" effects not significant). Primary cilia of both cell types have 300 to 900 particles/μm^2.

At E18 and E19 putative ciliated cells tend to have higher particle densities than cells with secondary cilia (Fig. 25; Table 1, X). Also, and in contrast to cells with primary cilia (Table 1, IX, "age" effect not significant), respiratory cells with secondary cilia display an age effect. This is caused by the high densities in P-faces of microvilli of ciliated cells in adults (Fig. 25; Table 1, XI, XII). Apices of cells with secondary cilia have 300 to 700 particles/μm^2, their microvilli 200 (at E18) to 1800 (adults; Fig. 25) and the secondary cilia themselves about 400 particles/μm^2. I also examined whether shorter secondary respiratory cilia differ from longer ones in their particle density. For this, cilia were ranked according to necklace strand numbers. Longer cilia tend to have more strands than shorter cilia

Fig. 4. E14.2 olfactory epithelial surface fractured parallel to that surface. All cells display P-faces. Round olfactory receptor cell dendritic endings are present amidst large olfactory supporting cell expanses. One receptor cell displays a primary cilium (*large arrow*). Two endings without cilia are marked with *large arrowheads*. Apices of supporting cells have ample microvilli (*small arrowheads*) and, sometimes, a primary cilium (*small arrow*) and globular particles. × 20000

Fig. 5. Two clustered E16 olfactory receptor cell dendritic endings, without cilia. One demonstrates a P-face (*left*), the other an E-face. The tight-junctional belt interconnecting the endings displays an intricate lacework. × 95000

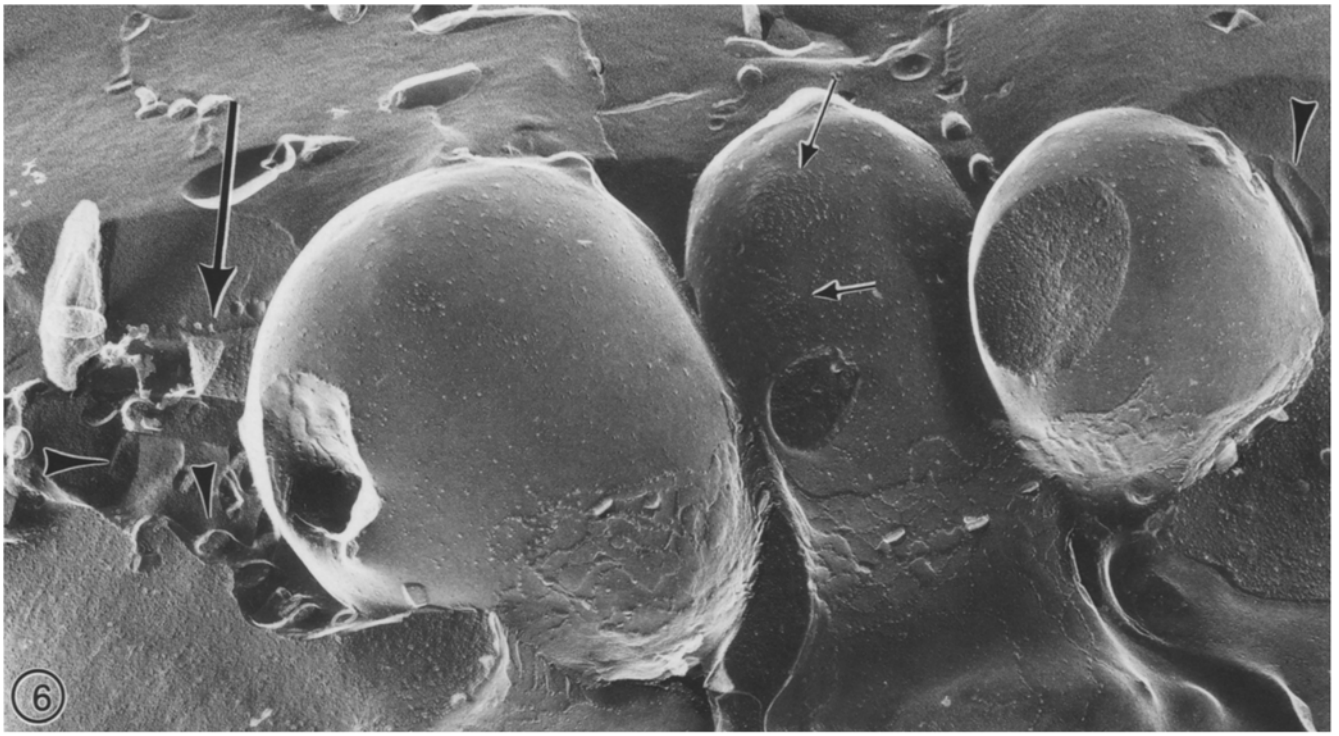
6

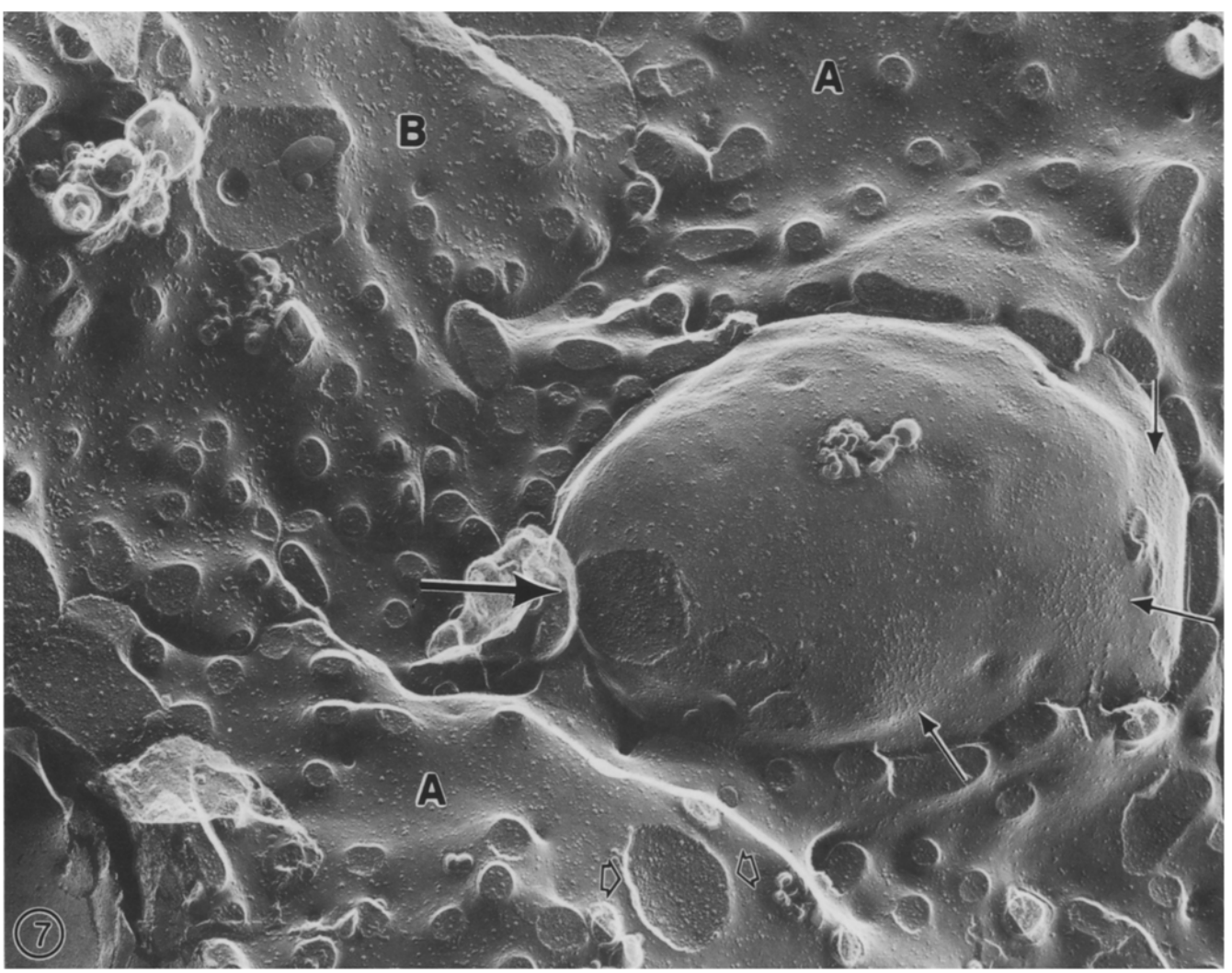
A
B
A
7

during development (Menco 1988b). Grouping particle densities of cilia with 1–2, 3–4, and 5–6 necklace strands, I found that particle densities are independent of ciliary length. However, young respiratory cilia have some large particles in their P-faces (Figs. 21, 22) that were not encountered in mature respiratory cilia.

Comparing receptor cells with supporting cells and with respiratory cells

Structures of distal regions of olfactory receptor and supporting cells and of putative ciliated and ciliated respiratory cells were considered to be analogous for a comparison of their particle densities as a function of developmental age (Figs. 23–25). Fig. 25 is rather flat; that is, there is no systematic increase in particle densities with age after E14 for respiratory cells, whereas densities increase with age in olfactory receptor and supporting cells (Figs. 23, 24; Table 1, III, V, VI, and VII contain "age" effects; IX and X lack "age" effects). Comparisons of pairs (not presented) emphasize this. The pattern is maintained in adults. From E16 on olfactory receptor cell endings have lower densities than apical structures of supporting cells. Adult values are reached at E17 in the latter cells; receptor cells reach these at E18 (Figs. 23, 24).

Overall particle densities in apical structures of the three cell types differ significantly from E16 on but not at E14.1 and E14.2 (Figs. 23–25; Table 2, I, "cell type"). Also, densities in supporting cell and putative ciliated respiratory cell microvilli are higher than densities in apices and primary cilia of these cells (Figs. 24, 25). These differences are the cause of the P-face structure effects for age groups E14.2 through E18 in Table 2, I.

Comparing Figs. 23 through 25 suggests that particle densities in apical regions of microvillous respiratory cells are also lower than those in olfactory receptor and supporting cells. Apical regions of microvillous respiratory cells and of Type B olfactory supporting cells have dumbbell-shaped particles; these are present in higher densities in the supporting cells (Figs. 7, 15, 19, 20). Primary cilia of both cell types (Figs. 15, 19, 24, 25; Table 1, VIII) and also of vomeronasal supporting cells (Fig. 11, Menco 1988b) tend to have lower particle densities than apices and microvilli.

Primary and secondary cilia

Primary cilia are usually found at luminal surfaces of epithelial cells (Figs. 1, 2, 4, 6, 7, 14–19), but they are sometimes present in intercellular spaces (Fig. 3). They were seen in all undifferentiated (Figs. 1–3) and differentiating cell types (Figs. 4–7, 14–19) encountered in this study. Occasionally they were also seen on olfactory basal cells, vomeronasal sensory and supporting cells, and on cells lining ducts of Bowman's glands (Menco 1988b). Primary cilia are often conical for about 0.3 μm, ending in a short stalk (about 0.7 μm; Figs. 17–19; Figs. 1, 6, 7, Menco 1988b). Especially at E14.1, but also later on, they can be surrounded by a plasma membrane pouch. Figs. 1–3 present the first freeze-fracture images of such pouches. Pouch shapes outline those of cilia inside; they display no special freeze-fracture features, apart from extracellular matrix arrays of particles in the region where the cilia emerge from these pouches (Fig. 8, Menco 1988b). Distributions of pouch intramembranous particles resemble those of the rest of the apical structures from which the cilia emerge. Particles tend to be homogeneously distributed in primary (Fig. 3; Fig. 9, Menco 1988b) and secondary olfactory cilia (Fig. 8) and in respiratory cilia (Figs. 21, 22), including shafts and expanded tips. An exception are the large particles of developing cilia of the latter cell type which seem to be present more closely to the base than elsewhere (Fig. 22).

Densities of intramembranous particles in primary cilia of olfactory receptor cells, olfactory supporting cells, and putative ciliated respiratory cells do not significantly differ (Fig. 26; Table 2, II, V, "cell types" not significant). Densities of primary cilia of nasal epithelial cell types not included in Fig. 26 (microvillous respiratory cells, olfactory basal cells, olfactory glandular cells, vomeronasal sensory and supporting cells) are within range of those of primary cilia of the cells presented in Fig. 26. There is wide variation from one cell to the next, however (compare Figs. 1 and 7, Menco 1988b).

P-face densities in membranes of primary cilia of olfactory receptor and respiratory cells differ significantly from those of secondary cilia (Table 2, III, IV). Secondary olfactory cilia tend to have higher densities than primary olfactory cilia (Figs. 23, 26); the reverse is true for primary and secondary respiratory cilia (Figs. 25, 26). Densities in membranes of primary and secondary cilia increase with age (Fig. 26; Table 2, II–V).

A key observation is that densities in membranes of developing secondary olfactory and respiratory cilia differ dramatically (Fig. 26; Table 2, VI). Membranes of olfactory cilia have considerably higher densities than membranes of respiratory cilia. This is true as soon as genesis of either secondary cilium type begins (Figs. 23, 25, 26). From E18 on, at which respiratory cilia begin to form, neither of them shows an increase in particle density (Table 2, VI, "age" effect not significant).

Discussion

During pre-natal development intramembranous particle densities increase much more dramatically in apical struc-

Fig. 6. A cluster of three E16 receptor cell dendritic endings displaying P-faces with low particle densities. One ending has a primary cilium in its necklace region (*large arrow*), another ending has areas of incipient cilium formation (*small arrows*; Menco 1980d). Some supporting cell microvilli are marked with *arrowheads*. The mucus (*area above endings*) is virtually devoid of distal cilium segments. × 40000

Fig. 7. E17 olfactory epithelial surface fractured parallel to that surface. All cells display P-faces. Supporting cells without (*A*) and with dumbbell-shaped (*B*) particles in their apices surround a dendritic ending of an olfactory receptor cell with a detached primary cilium (*large arrow*) and regions characteristic for incipient cilium formation (*small arrows*). Both supporting cell types have many profiles of microvilli. *Two open arrows* mark a supporting cell primary cilium removed during fracturing. × 50000

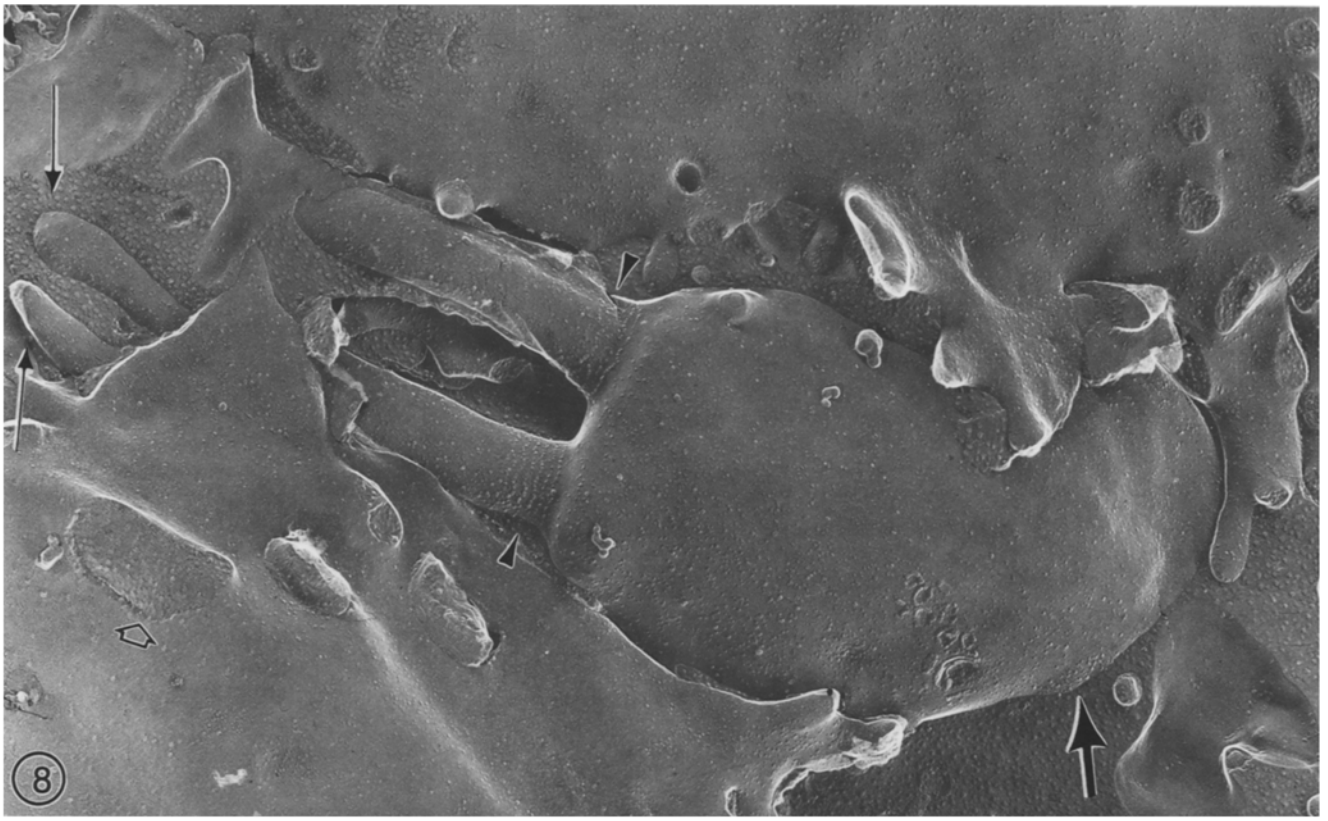
8

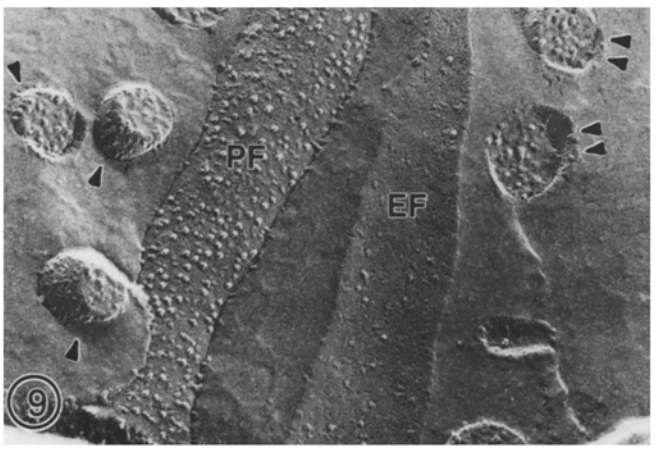
PF
EF
9

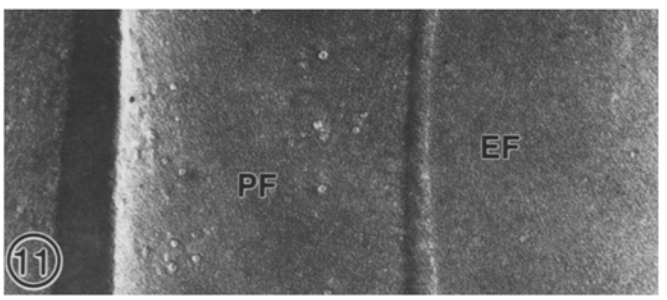
PF
EF
11

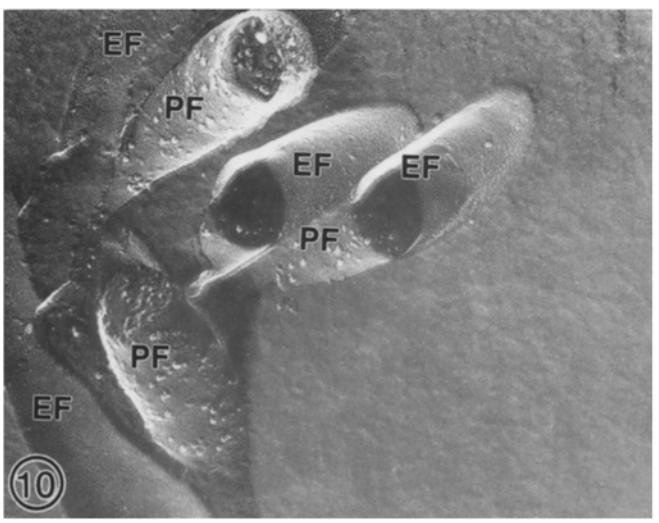
EF
PF
EF
EF
PF
PF
EF
10

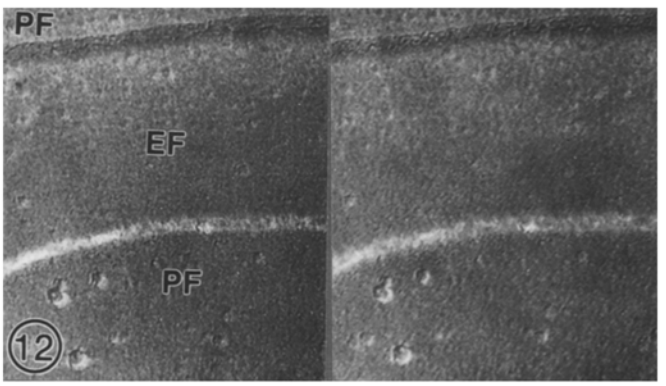
PF
EF
PF
12

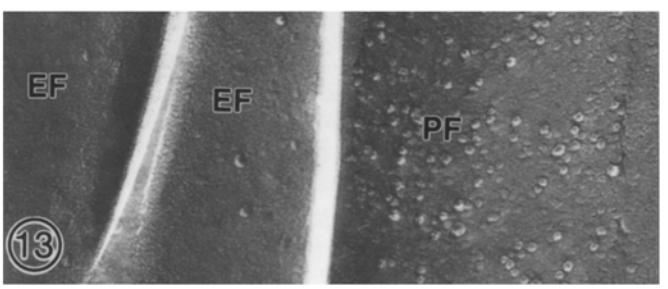
EF
EF
PF
13

tures of olfactory receptor and supporting cells than in those of nasal respiratory epithelial cells. Moreover, membrane-related morphological changes which take place during pre-natal development coincide with the time that the receptor cells acquire secondary cilia (Menco and Farbman 1985a, b) and become preferentially responsive to a limited set of odorants (Gesteland et al. 1982). The main function of olfactory cilia, and their membranes in particular, is their role as carriers of chemosensory receptor molecules and molecules involved in the initial transduction cascade of the odorous messages (Getchell 1986; Holley and Mac Leod 1977; Lancet 1986; Menco 1977, 1983). Mammalian olfactory cilia are most likely immotile and the axonemal cytoskeletal structures merely serve as carriers for the membranes (Lidow and Menco 1984; Menco and Farbman 1985c). Consequently, it is more than likely that the biochemical entities reflected as particles in secondary endings and in supporting cell apical structures play an important role in olfactory chemosensory receptor and/or transduction processes as, for example, ion-channel proteins (Nakamura and Gold 1987) and adenyl cyclase (Pace et al. 1985). Although the exact nature and function of the entities the particle represent is still unknown, we have preliminary evidence that some of the particles display pores, suggesting that these particles reflect transmembranous channels (Menco et al. 1988).

Cells with primary cilia

Freeze-fracture images on primary cilia presented here and in the accompanying paper (Menco 1988b) resemble those of primary cilia which can be see in three other publications. One of these gave only cross fractured bases of primary cilia of developing vestibular hair and supporting cells (Favre et al. 1986); the other two showed primary cilia of cultured chick fibroblasts (Gilula and Satir 1972) and retinal neuroblasts (Whiteley and Young 1985). Also, there is a remarkable resemblance between the freeze-fracture morphology of primary cilia and that of spermatozoan flagella of some invertebrates. The similarity includes the number of necklace strands (Cosson and Gulik 1982; Menco 1988b) and the presence of a membranous sac from which flagella (Cosson and Gulik 1982) and primary cilia emerge; in either case the membrane sacs do not demonstrate any special particle dispositions.

The transformation of primary dendritic endings into secondary ones

The one other study on the freeze-fracture morphology of developing olfactory receptor cells dealt with mice rather than rats and did not include olfactory supporting and respiratory cells (Kerjaschki 1977). Also, that investigation was not a day by day study and primary endings were not separated from secondary ones. Kerjaschki found that the olfactory receptor cell dendritic endings have about 250 particles/μm^2 when they are below the luminal surface, 850 particles/μm^2 when they appear above that surface, but lack cilia, and 1100 particles/μm^2 after they develop cilia. I did not study the endings when they are below the luminal surface, but otherwise Kerjaschki's (1977) values are similar to those presented here (Fig. 23). Densities in endings and cilia of adults match previous values (Breipohl et al. 1982; Kerjaschki and Hörandner 1976; Menco 1980b, 1983, 1984; Usukura and Yamada 1978). Secondary endings have larger surfaces than primary ones (Menco and Farbman 1985b). Hence, differences in particle distributions between primary and secondary endings (Figs. 23, 27; Table 1, II) become more explicit when densities are combined with ending surface areas (Fig. 28) or when they are examined per μm^2 epithelial surface (Fig. 29).

Because of two major sampling problems, the proportions of cells considered to have primary endings are too high. *Sampling error a*: Densities of endings with no cilia and endings with one cilium were pooled (labelled *Ending Pr* in Fig. 23). However, endings are almost never totally exposed in replicas. Some of the ending is not included in the fracture plane and/or is removed during the fracturing process (Fig. 6). Therefore, endings on which I saw no cilia might actually have had one (primary) or more cilia. If they had had one cilium they would still have belonged to the population of cells I considered to be primary. Endings on which I saw one cilium might in reality have had two or more cilia and were in that case erroneously considered to be primary. Endings with no cilia have significantly lower (data not shown) particle densities than endings with one visible cilium in age groups E16–E19 (Table 1, II, and especially IV, "structures"). This suggests that a considerable portion of the endings on which I saw one cilium and thus considered primary are, in fact, secondary endings. Compared to quantitative scanning electron microscopic

Fig. 8. E16 olfactory epithelial surface fractured parallel to that surface. All cells display P-faces with rather low particle densities. A dendritic ending displays proximal parts of two cilia having 4 and 6 necklace strands, respectively (*arrowheads*), and distal parts of two cilia (*small arrows*). One of the latter ones ends club-shaped (*small arrow pointing downward*). An area of incipient ciliogenesis is marked with a *large arrow*. Supporting cells have globular particles in their apices. The *open arrow* marks a supporting cell primary cilium removed during fracturing. × 40000

Fig. 9. High particle densities in P-faces (*PF*) of proximal parts of E19 secondary olfactory cilia. Surrounding supporting cell microvilli display P- (*one arrowhead*) and E-faces (*two arrowheads*). EF = E-faces cilia. × 100000

Fig. 10. High particle densities in P-faces (*PF*) of distal parts of E19 secondary olfactory cilia. EF = E-faces. × 100000

Fig. 11. P- (*PF*) and E-faces (*EF*) of E14.2 olfactory axons. × 150000

Fig. 12. Stereopair of P- (*PF*) and E-faces (*EF*) of E18 olfactory axons. In contrast to all other micrographs, which are made from platinum/carbov replicas this one is made from a tantalum/tungsten replica. × 150000

Fig. 13. P- (*PF*) and E-faces (*EF*) of axons of an adult rat. × 150000

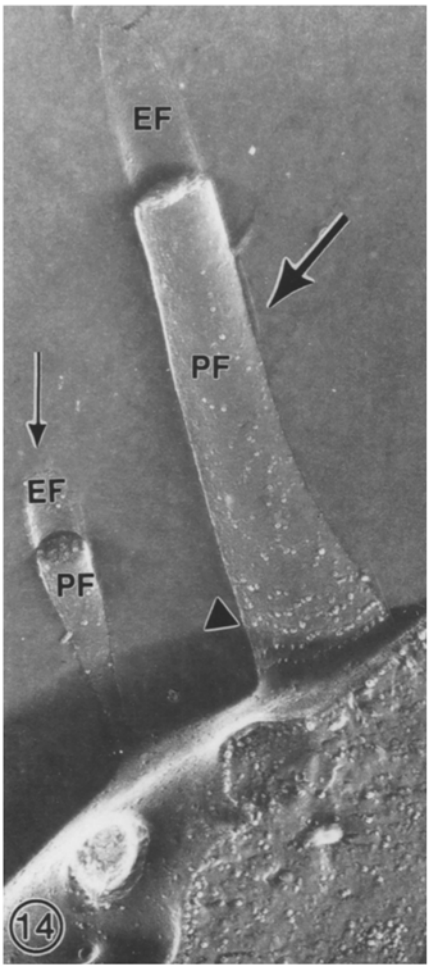
EF
PF
EF
PF
14

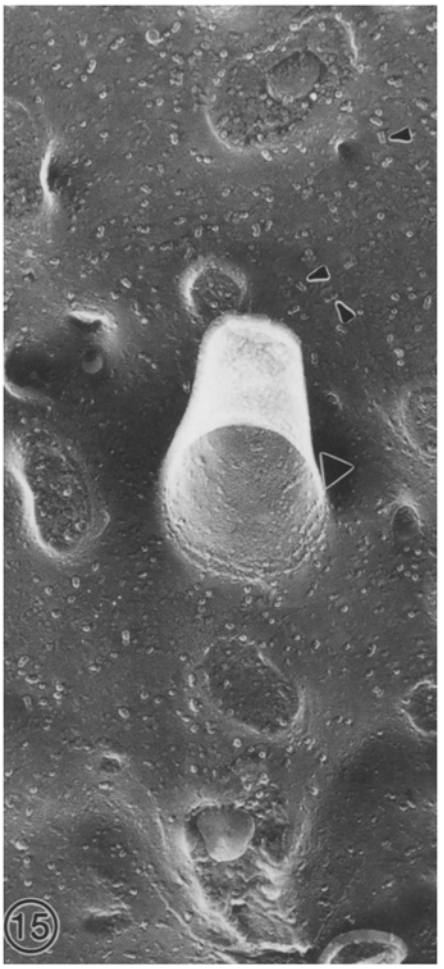
15

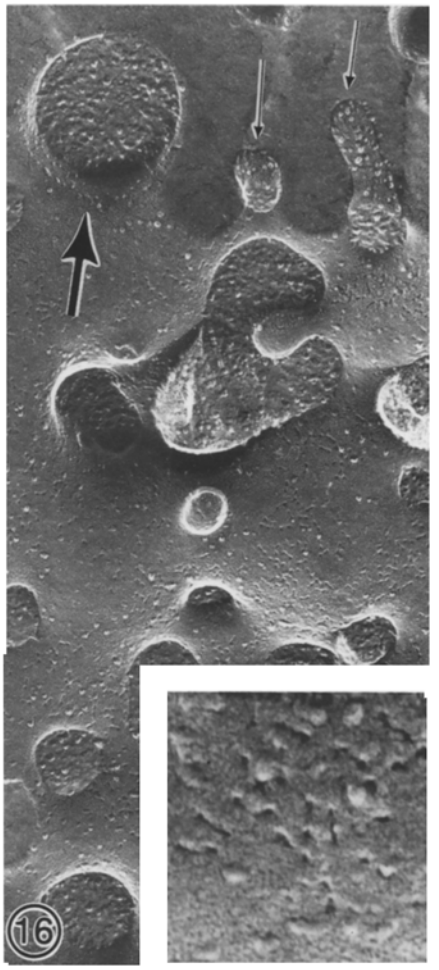
16

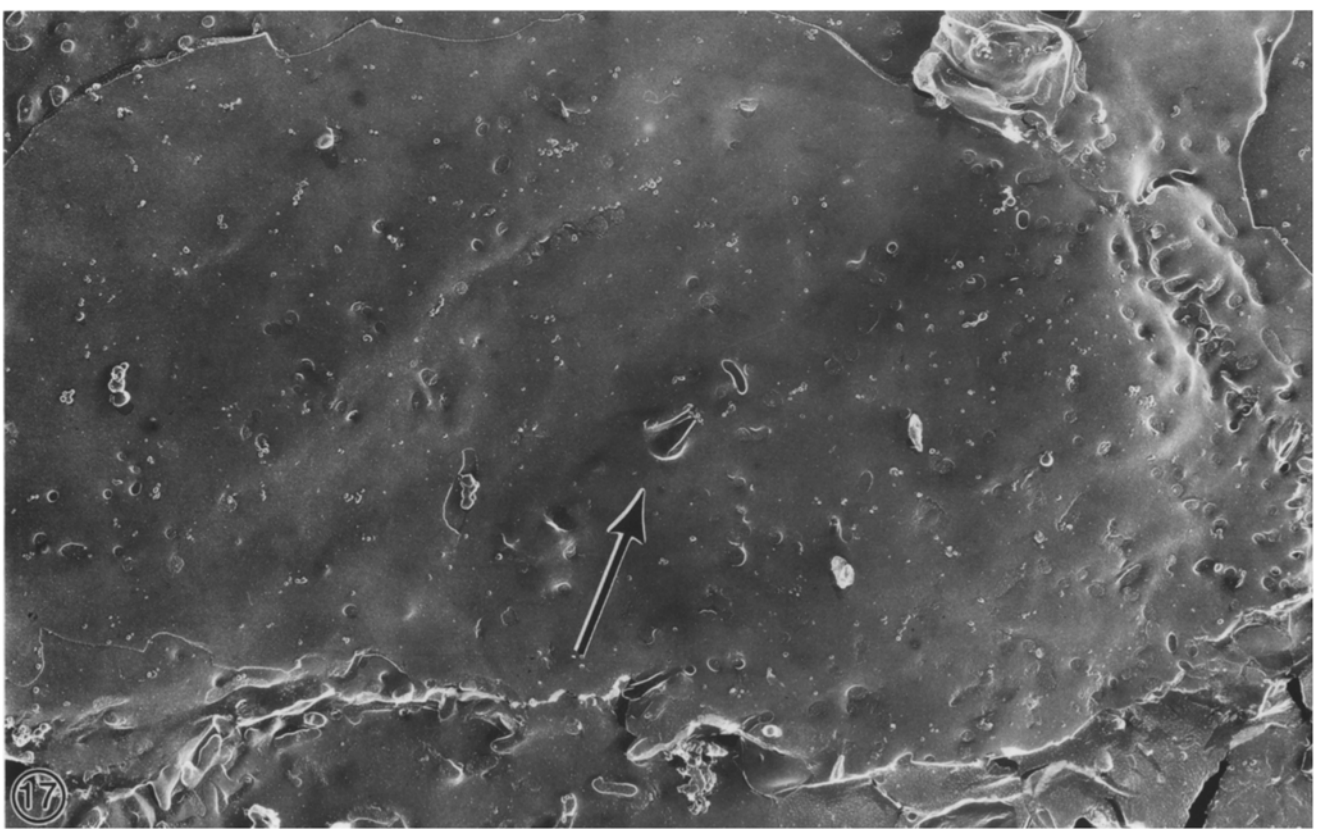
17

data (Menco and Farbman 1985b), I overestimated the fraction of primary endings by about 35%. *Sampling error b*: In the above mentioned scanning electron microscopic study, endings without cilia and endings with one cilium were considered to be primary. However, particle arrays characteristic for genesis of primary or secondary cilia cannot be seen with scanning electron microscopy. To be consistent with the scanning studies, I considered endings without cilia or with one cilium (Figs. 6, 7), but with one such particle array, as primary. In reality such cells are in an intermediate developmental stage. As a consequence of sampling errors *a* and *b* particle densities in primary endings are most likely lower than reported here resulting in larger density differences between primary and secondary endings (Figs. 23, 26–29; Table 1, II); it appears that particle densities increase mainly when the endings begin to sprout secondary cilia.

Olfactory cilia continue to sprout and grow after E19 (Menco and Farbman 1985a, b). Therefore, even though particle densities in secondary endings are established around E18 (Figs. 23, 27), absolute particle numbers continue to increase pre- and also post-natally. E18 and E19 secondary endings in embryos have only about 7% to 8% of the total number of particles found in adult samples (Fig. 28), whereas a 1 μm^2 epithelial area in the same embryos has 3% to 4% of the particles found in adults (Fig. 29).

Axonal features versus dendritic ending features

At E19, a time when many cells are already specifically receptive to odorants (Gesteland et al. 1982), olfactory receptor cell axons did not yet show an increase in densities of intramembranous particles (Fig. 23). Moreover, the earliest synapses of olfactory receptor cell axons were only seen at E18 (Farbman 1986; Farbman and Menco 1986). This emphasizes the notion that dendritic ending structures, rather than axons, are involved in the onset of odorant specificity. It is possible that the increase in axonal particle densities is due to the fact that the receptive surface areas of the olfactory dendritic endings continue to increase even after the densities in those compartments do no longer increase, i.e., after E18 (Figs. 27–29). My results on newly developing olfactory axons of rat embryos are supported by those on other unmyelinated axons (Black et al. 1983; Garcia-Segura and Perrelet 1981). Small and Pfenninger (1984) showed, in frogs, that after transection of the olfactory nerve, newly formed axons also have lower particle densities than mature ones. Olfactory receptor cell axolemmal densities in adults found here match values of Köling et al. (1986) and Menco (1980b), but not those of Small and Pfenninger (1984), in adult frogs, which are somewhat higher.

Membrane features of axons and dendritic endings of olfactory receptor cells display a differential developmental pattern (Fig. 23). Tight-junctions (Kerjaschki 1977; Kerjaschki and Hörandner 1976; Menco 1980c, 1988a) and the fact that both compartments are quite remote from each other might be partly responsible for this. Also, growing olfactory axons display a gradient with highest particle densities closest to the perikaryon (Small and Pfenninger 1984; Small et al. 1984).

Transformations in supporting cell apical structures

The species, animal strain, or sample having the highest densities in apical structures of olfactory receptor cells also has the highest densities in apical structures of supporting cells (Menco 1980b, 1983). I showed that this pattern apparently is established pre-natally (Figs. 23, 24), suggesting that both cell types interact at one or more levels, and recent physiological results support this supposition (Getchell et al. 1987). Particle densities in supporting cell apical structures of adults resemble values reported elsewhere (Breipohl et al. 1982; Menco 1980b, 1983, 1984).

Mammalian supporting cells belong in majority to one cell type which seems to be truly polymorphic. Dumbbell-shaped particles, characteristic for apices of Type B supporting cells, were found in mammalian olfactory supporting cells, cells lining ducts of glands of Bowman, and microvillous cells of the nasal respiratory epithelium (Hörandner et al. 1974; Menco 1980b, 1984). They were also found in other nasal epithelial cell types, including those of the septal olfactory organ (Miragall et al. 1984) and of vomeronasal olfactory supporting cells (Breipohl et al. 1982). Dumbbell-shaped particles in apical membranes tend to be accompanied by many mitochondria below these membranes (Brown et al. 1978; Menco 1983). Whereas supporting cells of adult mammals have mainly dumbbell-shaped membrane particles and many mitochondria in apical regions, immature supporting cells have few mitochondria (Cuschieri and Bannister 1975; reexamination of my own micrographs) and lack dumbbell-shaped particles (this study). The biochemical entities represented by the dumbbell-shaped particles most likely contain special factors required for a proper functioning of the olfactory epithelium. Mitochondria are needed to express those factors.

Polymorphism of mammalian olfactory supporting cells is expressed at various other levels, i.e., the shape of apices

Fig. 14. P- (*PF*) and E-faces (*EF*) of primary cilium (*large arrow*) and microvillus (*small arrow*) of an E14.2 Type A olfactory supporting cell. The ciliary necklace has 4 strands; the top one is incomplete (*arrowhead*). ×75000

Fig. 15. P-face of an E17 Type B olfactory supporting cell primary cilium. The apex has a higher particle density than the cilium and also some dumbbell-shaped P-face particles (*small arrowheads*) in contrast to the cilium. The ciliary necklace has 2–3 strands; the top one is incomplete (*large arrowhead*). Profiles of microvilli, removed during the fracturing process, surround the primary cilium. ×75000

Fig. 16. E-face of E19 Type B supporting cell apex with a primary cilium and its necklace (*large arrow*). The apex has dumbbell-shaped pits (*inset*), which are absent near the cilium. P-faces of some microvilli contain mainly globular particles and a few dumbbell-shaped ones (*small arrows*). ×75000; inset: ×300000

Fig. 17. E-face of E16 putative ciliated respiratory cell with a conical primary cilium (*arrow*) and some microvilli. ×15000

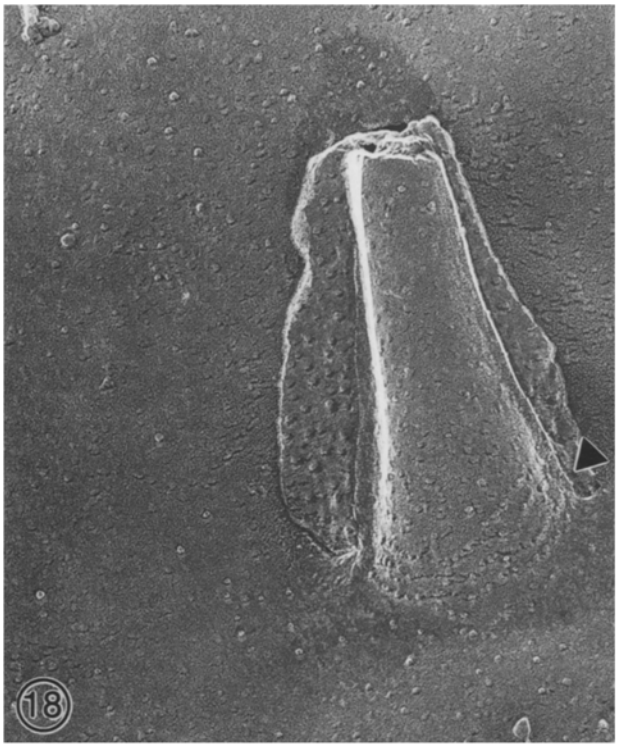

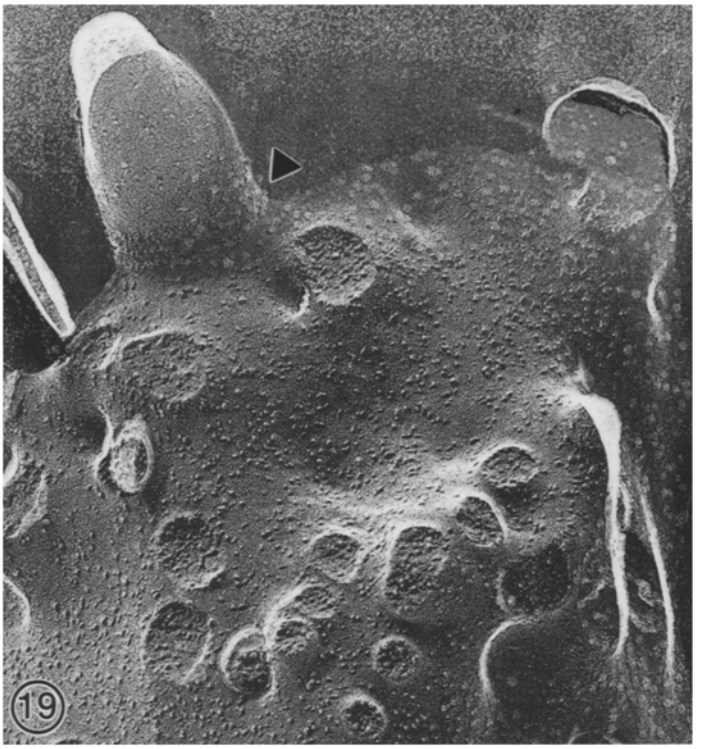

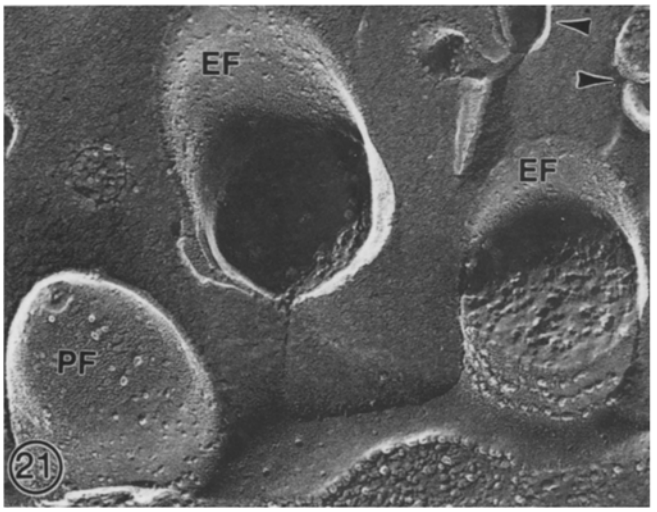
EF
EF
PF

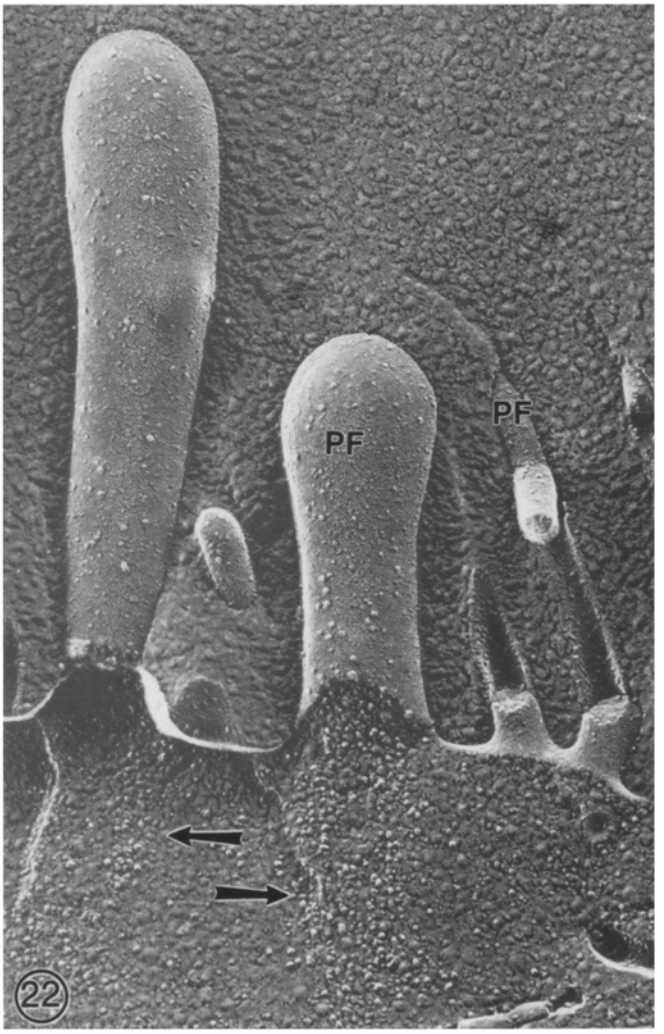
PF
PF

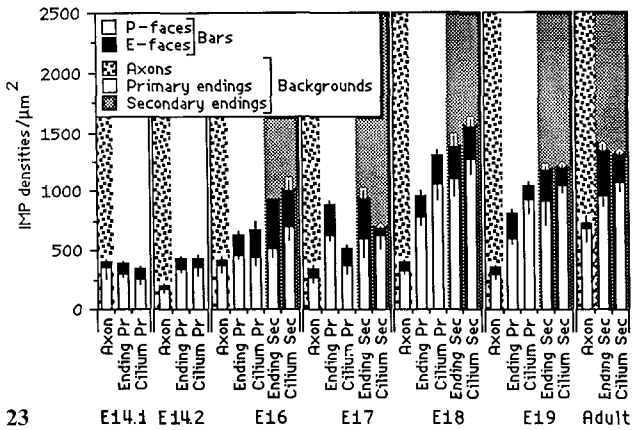

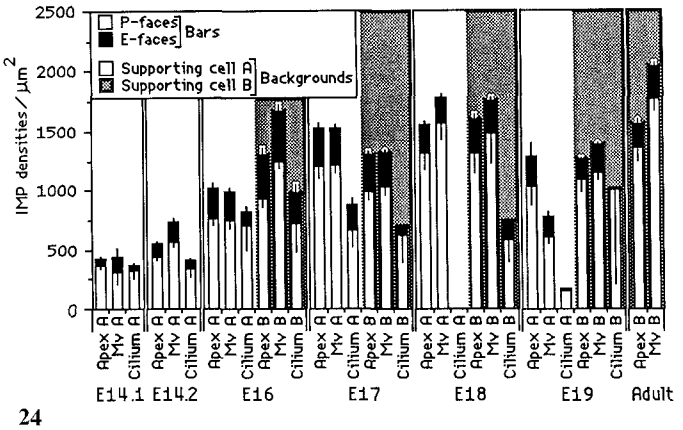

Fig. 23. Histograms of intramembranous particle densities in P- and E-faces of axons, and in dendritic endings and cilia of olfactory receptor cells in rat embryos and in adults. Bars mark standard errors; those of P-faces point downward, those of E-faces upward. Other statistics are presented in Tables 1 and 2. *IMP*, intramembranous particles; *Ending Pr*, primary endings; *Ending Sec*, secondary endings; *Cilium Pr*, primary cilia; *Cilium Sec*, secondary cilia

Fig. 24. Intramembranous particle densities in P- and E-faces of Types A and B olfactory supporting cells in rat embryos and in adults. Bars mark standard errors; those of P-faces point downward, those of E-faces upward. Other statistics are presented in Tables 1 and 2. *IMP*, intramembranous particles; *Apex*, apices from which microvilli and primary cilia originate; *Mv*, microvilli; *Cilium*, primary cilia

and the length of the microvilli. Those polymorphic features may partly be due to environmental and physiological conditions (Menco and Farbman 1985a). Amphibians have also two types of supporting cells, but these may really represent two different cell types (Rafols and Getchell 1983; Trotier and Mac Leod 1986) and not be due to polymorphism of one cell type as is the case here in mammals. Also, apices of frog supporting cells differ from those of mammals in that they have hardly any dumbbell-shaped particles and are massively filled with secretory vacuoles rather than mitochondria (Menco 1980b).

Genesis of secondary cilia and microvilli in the respiratory epithelium

In contrast to secondary olfactory cilia where particle densities increase with development, densities in respiratory cilia resemble those in adults as soon as genesis of secondary cilia begins, from E18 on. As microvilli of ciliated respiratory cells have lower particle densities in embryos than in adults (Figs. 25, 26; Menco 1980b, 1983, 1984), these cell appendages apparently obtain their full complement of particles at a stage when all cilia are aligned and motile (Menco and Farbman 1987). Particle densities of respiratory cilia remain also more or less constant throughout development in mice, and this pattern continues post-natally (Lessner and Rehn 1987), although, the density values given by these investigators are about five times higher than those found by Kerjaschki and Hörandner (1976), also in mice, and those found here in the rat. Moreover, Lessner and Rehn (1987) found that the particles display a density dip one day before birth, a day not included in this investigation.

My results (Fig. 25) are in partial agreement with those of Chailley and Boisvieux-Ulrich (1985) on bird oviduct ciliated cells where membranes of cilia and microvilli differ, especially regarding the disposition of cholesterol probes. This is true when the cells develop and when they are mature. However, whereas I found that there are no differences in densities as a function of ciliary length, Chailley et al. (1982, 1983) found that kinocilia have higher particle densities at the onset of ciliogenesis than later on when they are longer. Also in contrast with those authors, I found that particle densities are the same in both shafts and tips of developing respiratory cilia, not higher in the tips.

Fig. 18. P-face of a conical E16 primary cilium, with 4 necklace strands (*arrowhead*), of a putative ciliated respiratory cell. × 100000

Fig. 19. P-face of apex with conical primary cilium displaying 3 necklace strands (*arrowhead*) of an E16 microvillous respiratory cell. The cilium has a lower particle density than the apex, which has also some dumbbell-shaped particles. × 75000

Fig. 20. P-face of apices of ciliated (*left*) and microvillous (*right*) respiratory cells in an E19 embryo. The apex of the microvillous cell bulges and contains some dumbbell-shaped particles. × 30000

Fig. 21. Genesis of secondary respiratory cilia and of microvilli (*arrowheads*) in an E19 embryo. Cilia are short, have few particles in P- (*PF*) and E-faces (*EF*), and 1 to 3 necklace strands. × 100000

Fig. 22. Genesis of secondary respiratory cilia (P-faces) in an E19 embryo. The cilia are bat-shaped, somewhat longer than those in Fig. 21, and still contain only a few particles, which can be rather large. Etching exposed basal body outlines (*arrows*). Microvillous P-faces also have few particles. × 75000

Table 1. Summarized statistics on intramembranous particle densities of developing olfactory receptor (Fig. 23) and supporting cells (Fig. 24), and of nasal respiratory cells (Fig. 25).

Figure numbers and the compared age groups, cell types, and structures[a]	Significant effects	Three way ANOVAs			Two way ANOVAs			One way ANOVA		
		F	df	*p*<	*F*	df	*p*<	*F*	df	*p*<
I. Fig. 23. *Axons*: E14.1 through adult	Ages: P-faces							6.47	6,177	0.0001
II. *Receptor cells*: Primary/secondary; E16 through E19; endings/cilia	Primary/secondary: P-faces	13.36	1	0.0005						
	E-faces	5.51	1	0.05						
	Ages: P-faces	23.68	3	0.0001						
	Structures: P-faces	4.53	1	0.05						
III. *Receptor cells, primary*: E14.1 through E19; endings/cilia	Ages: P-faces				23.88	5	0.0001			
	E-faces				7.88	5	0.0001			
	Interactions: ages-structures: P-faces				6.76	5	0.0001			
	E-faces				2.90	5	0.05			
IV. *Receptor cells, primary*: E14.1 through E19; no cilia/one cilium (pooled in Fig. 23)	Ages: P-faces				17.47	5	0.0001			
	E-faces				15.63	5	0.0001			
	Structures: P-faces				6.58	1	0.05			
	Interactions: ages-structures: P-faces				7.83	5	0.0001			
	E-faces				4.86	5	0.0005			
V. *Receptor cells, secondary*: E16 through adult; endings/cilia	Ages: P-faces				6.00	4	0.0001			
	Structures: E-faces				5.19	1	0.05			
VI. Fig. 24. *Supporting cells*: Supporting cells without dumbbell-shaped particles (Type A) in their a pices/supporting cells with dumbbell-shaped particles (Type B) in their apices; E16 through E19; apices/microvilli[b]	Type A/Type B: P-faces	4.27	1	0.05						
	E-faces	4.36	1	0.05						
	Ages: P-faces	19.05	3	0.0001						
	E-faces	5.51	3	0.001						
	Interactions: Types A/B-ages: P-faces	9.19	3	0.0001						
	E-faces	4.05	3	0.01						
	Types A/B-structures: P-faces	4.25	1	0.05						
	Ages-structures: P-faces	2.83	3	0.05						
VII. *Supporting cells Type A*: E14.1 through E19; apices/cilia/microvilli	Ages: P-faces				14.57	5	0.0001			
	E-faces				4.95	5	0.0005			
VIII. *Supporting cells Type B*: E16 through adult; apices/cilia/microvilli	Structures: P-faces				4.43	2	0.05			
IX. Fig. 25. *Respiratory cells*: Putative ciliated respiratory cells/microvillous respiratory cells; E16 through E19; apices/microvilli[b]	Putative ciliated cells/microvillous cells: P-faces	13.13	1	0.0005						
X. *Respiratory cells*[c]: Primary/secondary; E18 through E19; apices/cilia/microvilli	Primary/secondary: P-faces	11.51	1	0.001						
	Interactions: primary/secondary-ages: P-faces	7.12	1	0.01						
	E-faces	8.87	1	0.005						
XI. *Respiratory cells with secondary cilia*: E18 through adult; apices/cilia/microvilli	Ages: P-faces				12.70	2	0.0001			
	Structures: P-faces				8.60	2	0.0005			
	Interactions: ages-structures: P-faces				9.96	4	0.001			
	E-faces				3.24	4	0.05			
XII. *Respiratory cells with secondary cilia*: E18 through adult; apices/cilia	Ages: P-faces				4.06	2	0.05			

[a] The beginning of a block is marked by a bold-printed figure number, the ends by dashed lines. Features on which the comparisons were performed are printed in italics
[b] Primary cilia were excluded from these comparisons, as these were not found in all age groups
[c] These comparisons deal only with putative ciliated and ciliated respiratory cells

Table 2. Summarized statistics on intramembranous particle densities of olfactory receptor cells, olfactory supporting cells and nasal respiratory cells over developmental age groups E14.1 through E19 and adults (Figs. 23–25), and of the cilium types of these cells (Fig. 26).

Figure numbers, and the compared age groups, cell types, and structures[a, b]	Effects	Two way ANOVAs		
		F	df	*p*<
I. Figs. 23–25. *E14.1 through adult*: Olfactory receptor cells/olfactory supporting cells/respiratory cells (=cell types); apices/cilia/microvilli (=structures)	E14.2, structures: P-faces	6.75	2	0.005
	E-faces	7.33	2	0.0001
	E16, cell types: P-faces	12.21	2	0.0001
	E16, structures: P-faces	4.06	2	0.05
	E17, cell types: P-faces	12.80	2	0.0001
	E17, structures: P-faces	5.41	2	0.01
	E18, cell types: P-faces	4.67	2	0.05
	E18, structures: P-faces	3.86	2	0.05
	E19, cell types: P-faces	23.33	2	0.0001
	Interaction: cell types-structures: P-faces	4.86	4	0.001
	Adult, cell types[c]: P-faces	4.19	2	0.05
	E-faces	6.80	2	0.005
II. Fig. 26. *Primary cilia*: Olfactory receptor cells/olfactory supporting cells/respiratory cells; E14.1 through E19	Ages: P-faces	4.06	5	0.005
	E-faces	4.88	5	0.0005
III. *Olfactory receptor cells*: E16 through E19; primary cilia/secondary cilia	Ages: P-faces	14.38	3	0.0001
	E-faces	3.14	3	0.05
	Primary/secondary: P-faces	6.68	1	0.05
IV. *Respiratory cells*: E16 through E19; primary cilia/secondary cilia	Ages: E-faces	4.84	3	0.005
	Primary/secondary: P-faces	14.15	1	0.0005
V. *Primary cilia*: Olfactory receptor cells/respiratory cells; E14.1 through E19	Ages: P-faces	6.20	5	0.0001
	E-faces	4.34	5	0.005
	Interaction: cell types-ages: P-faces	2.81	5	0.05
VI. *Secondary cilia*: Olfactory receptor cells/respiratory cells; E18 through adult	Cell types: P-faces	82.86	1	0.0001
	E-faces	9.63	1	0.005

[a] The beginning of a block is marked by a bold-printed figure number, the ends by dashed lines. Features on which the comparisons were performed are printed in italics

[b] Cells with primary and secondary cilia were pooled for these comparisons; supporting cells Types A and B were also pooled and only putative ciliated and ciliated respiratory cells were included; microvillous respiratory cells were not included

[c] Microvilli were excluded as inclusion of these gave too many missing statistical cells

Freeze-fracture developmental data versus data obtained with other techniques

Various biochemical and cytochemical changes take place simultaneously with the transient change that occurs when the receptor cells form secondary cilia (Carr et al. 1988; Farbman 1986; Farbman et al. 1987; Farbman and Menco, 1986; Mania-Farnell and Farbman 1987; Margolis et al. 1986; Menco and Farbman 1985b; Morgan 1986). However, it is unlikely that any of the factors listed in the above mentioned papers are expressed as intramembranous particles in embryos or in adults. Factors which are only found in olfactory receptor cells, in particular olfactory marker protein or OMP (Margolis et al. 1986; Morgan 1986), are cytoplasmic. None of the membrane-associated factors listed in the above publications is typical only for membranes of dendritic endings and cilia of olfactory receptor cells, apical structures of olfactory supporting cells, or apical structures of respiratory cells; all of them bind to more than one cell type and/or cellular region (Carr et al. 1988; Lidow et al. 1987). Nevertheless, functions of some of the biochemical and cytochemical factors might be closely related to functions of some of the factors expressed as intramembranous particles also as a function of development. Antibody 2B8 disappears from olfactory receptor cells with the appearance of OMP (Allen and Akeson 1985; Margolis et al. 1986), carnosine (Margolis et al. 1986, compare their Fig. 3 with Figs. 27–29 here) and GTP-binding proteins (Mania-Farnell and Farbman 1987). Binding sites for the lectin Con A appear (Smuts 1977) at a time when epithelial differentiation begins (Cuschieri and Bannister 1975). Antigens for antibodies 4A-5 and 3B-3 become expressed when respiratory cilia appear (Farbman et al. 1987).

Transient changes in particle densities as a function of development are also found in other biological systems. Such changes have been related to physiological and/or cytochemical properties of the system under investigation. Examples are microvilli of absorptive cells in mouse small intestine (Arima and Yamamoto 1983), rat retinal photoreceptors (Besharse et al. 1985) and acetylcholine receptors in cultured *Xenopus* embryonic muscles (Bridgman et al. 1984). Microvilli of the small intestine resemble those of

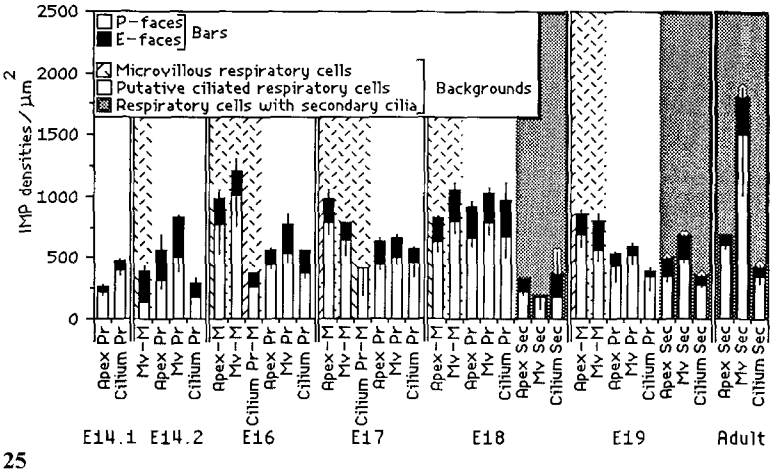

25

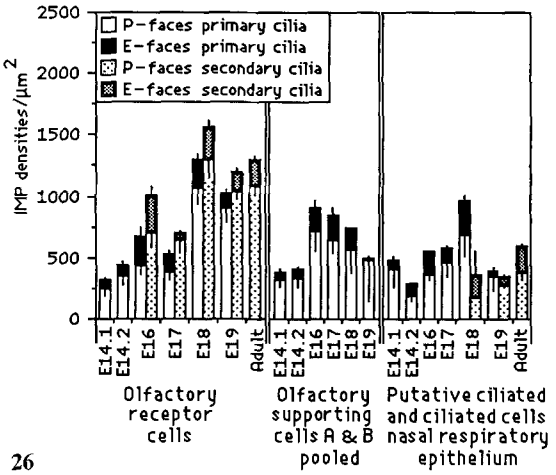

26

Fig. 25. Intramembranous particle densities in P- and E-faces of two types of nasal respiratory cells in rat embryos and in adults. Bars mark standard errors; those of P-faces point downward, those of E-faces upward. Other statistics are presented in Tables 1 and 2. *IMP*, intramembranous particles; *Apex Pr*, apices putative ciliated respiratory cells; *Mv Pr*, microvilli putative ciliated respiratory cells; *Cilium Pr*, primary cilia putative ciliated respiratory cells; *Apex-M*, apices microvillous respiratory cells; *Mv-M*, microvilli microvillous respiratory cells; *Cilium Pr-M*, primary cilia microvillous respiratory cells; *Apex Sec*, apices respiratory cells with secondary cilia; *Mv Sec*, microvilli respiratory cells with secondary cilia; *Cilium Sec*, secondary respiratory cilia

Fig. 26. Intramembranous particle densities in P- and E-faces of primary cilia of olfactory receptor, olfactory supporting, and putative ciliated respiratory cells and of secondary cilia of olfactory receptor and ciliated respiratory cells. Bars mark standard errors; those of P-faces point downward, those of E-faces upward. Other statistics are presented in Table 2. *IMP*, intramembranous particles

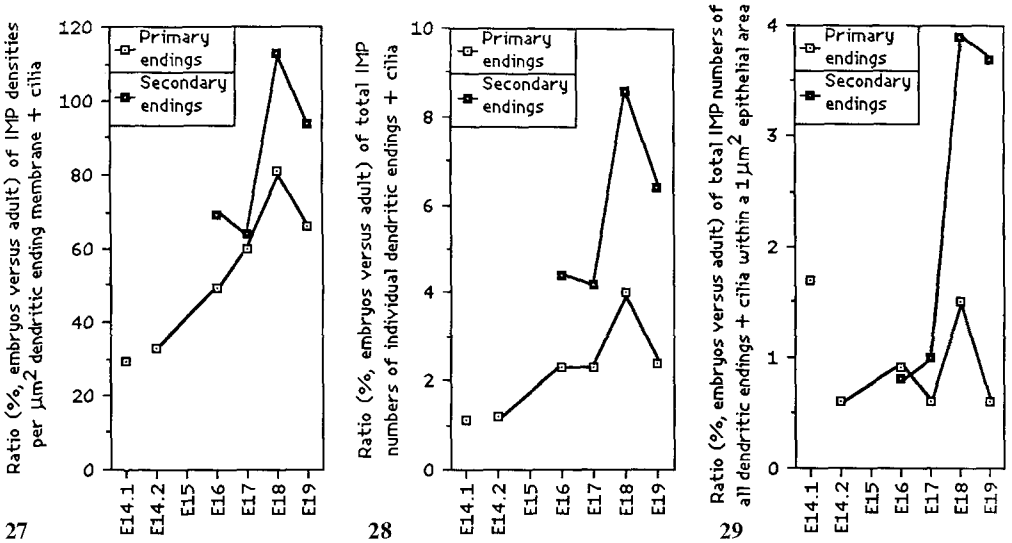

27

28

29

Fig. 27. Densities, pooled over P- and E-faces, of intramembranous particles per 1 μm^2 olfactory receptor cell dendritic ending membrane in embryos as percentage of that value in adults (1300 particles/μm^2). Endings include the cilia. Data points of age groups at which the cells differentiate are connected

Fig. 28. Total numbers, pooled over P- and E-faces, of intramembranous particles per olfactory receptor cell dendritic ending in embryos as percentage of that value in adults (2.84×10^5 particles/ending). Endings include the cilia. Membrane surfaces were obtained from Fig. 15 in Menco and Farbman (1985b). Data points of age groups at which the cells differentiate are connected

Fig. 29. Total numbers, pooled over P- and E-faces, of olfactory receptor cell dendritic ending intramembranous particles in embryos as percentage of that value in adults (1.9×10^4 particles/μm^2 epithelial area) above an epithelial surface area of 1 μm^2. Values include the cilia. Membrane expansions above 1 μm^2 epithelial areas were obtained from Fig. 16 in Menco and Farbman (1985b). Data points of age groups at which the cells differentiate are connected

olfactory supporting (Fig. 24) and respiratory epithelial cells (Fig. 25) in that they acquire more particles during development.

Finally, it seems that apices and microvilli of developing vomeronasal receptor and supporting cells also have lower densities in embryos (Figs. 10, 11, Menco 1988b) than in adults (Breipohl et al. 1982). My data were obtained from E19 embryos. That I still found low particle densities at that age is not surprising. Compared to the main olfactory organ, receptor processes of the vomeronasal olfactory organ have a developmental delay of several days (Taniguchi et al. 1982).

Acknowledgments. I am grateful to Drs. A.I. Farbman and F. Gonzales (Northwestern University) and to Audrey Niffenegger and Lyn Rosen for critical reading of this manuscript. Continuous technical support of Dr. P.A. Walley (Cressington Scientific, Watford, U.K.) and Mr. E.W. Minner was appreciated. This work was funded by NIH grant NS 21555.

References

Allen WK, Akeson R (1986) Identification of an olfactory receptor neuron subclass: Cellular and molecular analysis during development. Dev Biol 109:392–401

Arima T, Yamamoto T (1983) A freeze-fracture study of perinatal changes of intramembranous particles in microvilli of absorbtive cells in mouse small intestine. Cell Tissue Res 233:549–561

Besharse JC, Forestner DM, Defoe DM (1985) Membrane assembly in retinal photoreceptors. III. Distinct membrane domains in the connecting cilium of developing rods. J Neurosci 5:1035–1048

Black JA, Foster RE, Waxman SC (1983) Freeze-fracture ultrastructure of developing and adult non-myelinated ganglion cell axolemma in the retinal nerve fibre layer. J Neurocytol 12:201–212

Branton D, Bullivant S, Gilula NB, Karnovsky MJ, Moor H, Mühlethaler K, Northcote DH, Packer L, Satir B, Satir P, Speth V, Staehelin LA, Steere RL, Weinstein S (1975) Freeze-etching nomenclature. Science 190:54–56

Breipohl W, Mendoza AS, Miragall F (1982) Freeze-fracturing studies on the main and vomeronasal olfactory sensory epithelia in NMRI-mice. In: Breipohl W (ed) Olfaction and endocrine regulation. IRL Press Ltd, London, pp 309–322

Bridgman PC, Nakajima AS, Greenberg AS, Nakajima Y (1984) Freeze-fracture and electrophysiological studies of newly developed acetylcholine receptors in *Xenopus* embryonic muscle cells. J Cell Biol 98:2160–2173

Brown D, Ilic V, Orci L (1982) Rod-shaped particles in the plasma membrane of the mitochondria-rich cell of the amphibian epidermis. Anat Rec 192:269–275

Carr VMcM, Farbman AI, Colletti LM, Lidow MS, Hempstead JL, Morgan JI (1988) Developmental expression of reactivity to monoclonal antibodies generated against olfactory epithelia. J Neurosci (in press)

Chailley B, Boisvieux-Ulrich E (1985) Detection of plasma membrane cholesterol by filipin during microvillogenesis and ciliogenesis in quail oviduct. J Histochem Cytochem 33:1–10

Chailley B, Boisvieux-Ulrich E, Sandoz D (1982) Ciliary membrane events during ciliogenesis of the quail oviduct. Biol Cell 46:51–64

Chailley B, Boisvieux-Ulrich E, Sandoz D (1983) Evolution of filipin-sterol complexes and intramembrane particle distribution during ciliogenesis. J Submicrosc Cytol 15:275–280

Cosson MP, Gulik A (1982) Description of the mitochondria-axoneme junction in sea urchin spermatozoa: Presence of a flagellar necklace. J Ultrastruct Res 79:47–57

Cuschieri A, Bannister LH (1975) The development of the olfactory mucosa in the mouse: electron microscopy. J Anat 119:471–498

Farbman AI (1986) Prenatal development of mammalian olfactory receptor cells. Chem Sens 11:3–18

Farbman AI, Carr VMcM, Morgan JI, Hempstead JL (1987) Immunofluorescent studies of the development of rat olfactory epithelium. Ann NY Acad Sci 510:271–272

Farbman AI, Menco BPhM (1986) Development of olfactory epithelium in the rat. In: Breipohl W (ed) Ontogeny of olfaction. Principles of olfactory maturation in vertebrates. Springer, Berlin Heidelberg New York, pp 45–56

Favre D, Bagger-Sjöback D, Mbiene J-P, Sans, A (1986) Freeze-fracture study of the vestibular hair cell surface during development. Anat Embryol 175:69–76

Garcia-Segura LM, Perrelet A (1981) Freeze-fracture of developing plasma membrane in postnatal cerebellum. Brain Res 208:19–33

Gesteland RC, Yancey RA, Farbman AI (1982) Development of olfactory receptor neuron selectivity in the rat fetus. Neuroscience 7:3127–3136

Getchell ML, Zielinski B, DeSimone JA, Getchell TV (1987) Odorant stimulation of secretory and neural processes in the salamander olfactory mucosa. J Comp Physiol A 160:155–168

Getchell TV (1986) Functional properties of vertebrate olfactory receptor neurons. Physiol Rev 66:772–818

Gilula NB, Satir P (1972) The ciliary necklace. A ciliary membrane specialization. J Cell Biol 53:494–509

Holley A, Mac Leod P (1977) Transduction et codage des informations olfactives chez les vertébrés. J Physiol (Paris) 73:725–848

Hörandner H, Kerjaschki D, Stockinger L (1974) Rodshaped particles in epithelial free surface membranes. In: Sanders JV, Goodchild DJ (eds) Proceedings eighth international congress on electron microscopy, vol II. Australian Academy of Sciences, Canberra, pp 210–211

Karnovsky MJ (1965) A formaldehyde-glutaraldehyde fixative of high osmolarity for use in electron microscopy. J Cell Biol 27:137–138

Kerjaschki D (1977) Some freeze-etching data on the olfactory epithelium. In: Le Magnen J, Mac Leod P (eds) Olfaction and taste VI. Information Retrieval, London, pp 75–85

Kerjaschki D, Hörandner H (1976) The development of mouse olfactory vesicles and their contacts: A freeze-etching study. J Ultrastruct Res 54:420–444

Köling A, Rask-Andersen H, Deuschl H (1986) A freeze-fracture study of receptor axons and Schwann cells in the human olfactory mucosa. Acta Otolaryngol (Stockh) 102:494–499

Lancet D (1986) Vertebrate olfactory reception. Ann Rev Neurosci 9:329–355

Lessner U, Rehn B (1987) Ultrastructural analysis of the mouse nasal septum. Respiratory cilia prior to and after birth. A quantitative freeze-fracture study. Acta Anat 130:232–236

Lidow MS, Menco BPhM (1984) Observations on axonemes and membranes of olfactory and respiratory cilia in frogs and rats using tannic acid-supplemented fixation and photographic rotation. J Ultrastruct Res 86:18–30

Lidow MS, Farbman AI, Morgan JI, Hempstead J (1987) In vivo and in vitro studies of the localization of antigens recognized by monoclonal antibodies Neu-4, Neu-5 and Neu-9 in rat olfactory epithelium. Chemsens 12:676

Mania-Farnell B, Farbman AI (1987) Immunohistochemical localization of GTP-binding protein in rat olfactory epithelium during prenatal development. Chemsens 12:678

Margolis, FL, Kawano T, Grillo M (1986) Ontogeny of carnosine, olfactory marker protein and neurotransmitter enzymes in olfactory bulb and olfactory mucosa of the rat. In: Breipohl W (ed) Ontogeny of olfaction. Principles of olfactory maturation in vertebrates. Springer, Berlin Heidelberg New York, pp 107–116

Menco BPhM (1977) A qualitative and quantitative investigation of olfactory and nasal respiratory mucosal surfaces of cow and sheep based on various ultrastructural and biochemical techniques. Commun Agricult Univ Wageningen 77-13:1–157

Menco BPhM (1980a) Qualitative and quantitative freeze-fracture studies on olfactory and nasal respiratory structures of frog, ox, rat, and dog. I. A general survey. Cell Tissue Res 207:183–209

Menco BPhM (1980b) Qualitative and quantitative freeze-fracture studies on olfactory and nasal respiratory epithelial surfaces of frog, ox, rat, and dog. II. Cell apices, cilia, and microvilli. Cell Tissue Res 211:5–30

Menco BPhM (1980c) Qualitative and quantitative freeze-fracture studies on olfactory and nasal respiratory epithelial surfaces of frog, ox, rat, and dog. III. Tight-junctions. Cell Tissue Res 211:361–373

Menco BPhM (1980d) Qualitative and quantitative freeze-fracture studies on olfactory and nasal respiratory epithelial surfaces of frog, ox, rat, and dog. IV. Ciliogenesis and ciliary necklaces (Including high-voltage observations). Cell Tissue Res 212:1–16

Menco BPhM (1983) The ultrastructure of olfactory and nasal respiratory epithelium surfaces. In: Reznik G, Stinson SF (eds) Nasal tumors in animals and man, vol. 1, anatomy, physiology and epidemiology. CRC Press Inc, Boca Raton, Florida, pp 45–102

Menco BPhM (1984) Ciliated and microvillous structures of rat olfactory and nasal respiratory epithelia. A study using ultra-rapid cryo-fixation followed by freeze-substitution or freeze-etching. Cell Tissue Res 235:225–241

Menco BPhM (1986) A survey of ultra-rapid cryofixation methods with particular emphasis on applications to freeze-fracturing, freeze-etching, and freeze-substitution. J Electron Microsc Techn 4:177–240

Menco BPhM (1987a) A freeze-fracture study on the prenatal development of ciliated surfaces in rat olfactory epithelia. Ann NY Acad Sci 510:491–493

Menco BPhM (1987b) The freeze-fracture morphology of developing rat olfactory epithelium surfaces. Neuroscience: S130 [Abstr] 387P

Menco BPhM (1988a) Tight-junctional strands first appear in regions where three cells meet in differentiating olfactory epithelium. A freeze-fracture study. J Cell Sci 89:495–503

Menco BPhM (1988b) Pre-natal development of rat nasal epithelia. V. Freeze-fracturing on necklaces of primary and secondary cilia of olfactory and respiratory epithelial cells. Anat Embryol (in press)

Menco BPhM, Dodd GH, Davey M, Bannister LH (1976) Presence of membrane particles in freeze-etched bovine olfactory cilia. Nature 263:597–599

Menco BPhM, Farbman AI (1985a) Genesis of cilia and microvilli of rat nasal epithelia during pre-natal development. I. Olfactory epithelium, qualitative studies. J Cell Sci 78:283–310

Menco BPhM, Farbman AI (1985b) Genesis of cilia and microvilli of rat nasal epithelia during pre-natal development. II. Olfactory epithelium, a morphometric analysis. J Cell Sci 78:311–336

Menco BPhM, Farbman AI (1985c) Membranes versus cytoskeleton; their respective roles in olfactory reception. Chem Sens 10:391 [Abstr] 11

Menco BPhM, Farbman AI (1987) Genesis of cilia and microvilli of rat nasal epithelia during pre-natal development. III. Respiratory epithelium surface, including a comparison with the surface of the olfactory epithelium. J Anat 152:145–160

Menco BPhM, Minner EW (1986) Freeze-fracture studies on primary and developing secondary cilia of olfactory and nasal respiratory epithelia in rat fetuses. J Electron Microsc 35 [Suppl]:2601–2602

Menco BPhM, Minner EW, Farbman AI (1988) Preliminary observations on rapidly-frozen, freeze-fractured and deep-etched rat olfactory cilia rotary-replicated with tantalum/tungsten. J Electron Microsc Techn 8:441–442

Miragall F, Breipohl W, Naguro T, Voss-Wermbler G (1984) Freeze-fracture study of the plasma membranes of the septal organ of Masera. J. Neurocytol 13:111–125

Morgan JI (1986) Immunocytochemical studies on the maturation of the rodent olfactory mucosa. In: Breipohl W (ed) Ontogeny of olfaction. Principles of olfactory maturation in vertebrates. Springer, Berlin Heidelberg New York, pp 95–103

Nakamura T, Gold GH (1987) A cyclic nucleotide-gated conductance in olfactory receptor cilia. Nature 325:442–444

Pace U, Hanski E, Solomon Y, Lancet D (1985) Odorant-sensitive adenylate cyclase may mediate olfactory reception. Nature 316:255–258

Rafols JA, Getchell TV (1983) Morphological relations between the receptor cell neurons, sustentacular cells and Schwann cells in the olfactory mucosa of the salamander. Anat Rec 206:87–101

Small RK, Pfenninger KH (1984) Components of the plasma membrane of growing axons. I. Size and distribution of intramembrane particles. J Cell Biol 98:1422–1433

Small RK, Blank M, Ghez R, Pfenninger KH (1984) Components of the plasma membrane of growing axons. II. Diffusion of membrane protein complexes. J Cell Biol 98:1434–1443

Smuts MS (1977) Concanavalin A binding to the epithelial surface of the developing mouse olfactory placode. Anat Rec 188:29–37

Taniguchi K, Taniguchi K, Mochizoki K (1982) Comparative developmental studies on the fine structure of the vomeronasal sensory and the olfactory epithelia in the golden hamster. Jpn J Vet Sci 44:881–890

Trotier D, Mac Leod P (1986) Intracellular recordings from salamander olfactory supporting cells. Brain Res 374:205–211

Usukura J, Yamada E (1978) Observations on the cytolemma of the olfactory receptor cell in the newt. 1. Freeze replica analysis. Cell Tissue Res 188:83–98

Whiteley HE, Young S (1985) Cilia in the fetal and neonatal canine retina. Tissue Cell 17:335–340

Accepted December 23, 1987